

# Copper and zinc adsorption from bacterial biomass - possibility of low-cost industrial wastewater treatment

Diego Armando Santos Alves, Amilton Barbosa Botelho Junior, Denise Croce Romano Espinosa, Jorge Alberto Soares Tenório & Marcela dos Passos Galluzzi Baltazar

To cite this article: Diego Armando Santos Alves, Amilton Barbosa Botelho Junior, Denise Croce Romano Espinosa, Jorge Alberto Soares Tenório & Marcela dos Passos Galluzzi Baltazar (2023) Copper and zinc adsorption from bacterial biomass - possibility of low-cost industrial wastewater treatment, Environmental Technology, 44:16, 2441-2450, DOI: [10.1080/09593330.2022.2031312](https://doi.org/10.1080/09593330.2022.2031312)

To link to this article: <https://doi.org/10.1080/09593330.2022.2031312>



View supplementary material [↗](#)



Published online: 06 Feb 2022.



Submit your article to this journal [↗](#)



Article views: 222



View related articles [↗](#)






View Crossmark data [↗](#)



Citing articles: 4 View citing articles [↗](#)



## Copper and zinc adsorption from bacterial biomass - possibility of low-cost industrial wastewater treatment

Diego Armando Santos Alves, Amilton Barbosa Botelho Junior , Denise Croce Romano Espinosa , Jorge Alberto Soares Tenório  and Marcela dos Passos Galluzzi Baltazar

Department of Chemical Engineering, Polytechnic School, University of Sao Paulo, São Paulo, Brazil

### ABSTRACT

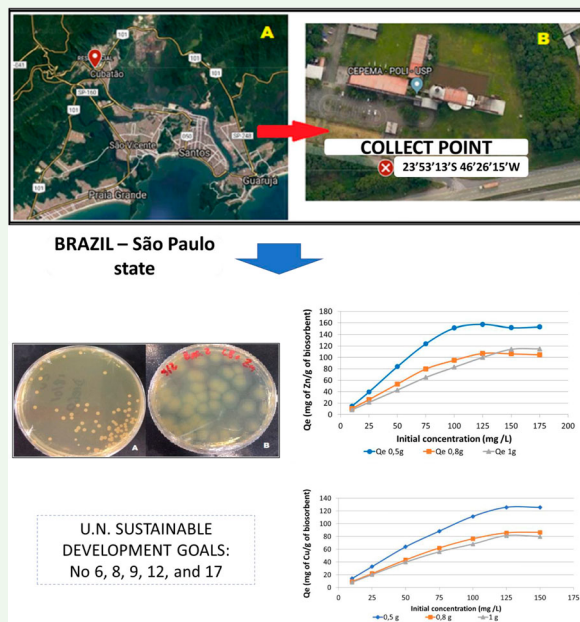
The increasing interest of all stakeholders to achieve environmental protection with socioeconomic development puts pressure on industrial processes for less negative impact on the environment. The use of biomass for wastewater treatment has increased due to its low costs and technical feasibility. The present study aimed the use of biomass from a waste of known polluted area for the adsorption of Zn and Cu in a fixed-bed reactor. Samples were collected in Cubatão (Brazil) and cultivated in LB medium. Resulting cultivable bacterial communities were identified as *Enterococcus faecalis* and *Pseudomonas aeruginosa*. Adsorption experiments were performed varying the metallic ion concentration and the amount of biomass. Adsorption experiments showed efficiency rates up to 90%. As the concentration of metallic ions increased, the adsorption efficiency decreased, indicating that the active sites were saturated. Activated charcoal demonstrated lower adsorption rates than biomass. Elution process showed that  $\text{HNO}_3$  had better efficiency than  $\text{HCl}$ . Zn adsorption fitted better for Lineweaver–Burk model ( $Q_{\text{max}} = 200 \text{ mg/g}$  of biomass), while Cu adsorption fitted better for Langmuir model ( $Q_{\text{max}} = 164 \text{ mg/g}$  of biomass). Results here demonstrated that the adsorption of Zn and Cu simulating an industrial wastewater by the biomass from a contaminated area is technically feasible.

### ARTICLE HISTORY

Received 27 October 2021  
Accepted 10 January 2022

### KEYWORDS


Adsorption isotherms;  
biosorption; Langmuir;  
Freundlich; SDGs




## 1. Introduction

The increase in environmental concerns and climate changes put pressure on industries and their stakeholders to develop a sustainable society. For this

reason, the United Nations launched in 2015 the 17 Sustainable Development Goals (U.N. SDGs) to be achieved in 2030. Guidelines for action on social inclusion, environmental sustainability, and economic

**CONTACT** Amilton Barbosa Botelho Junior  [amilton.junior@usp.br](mailto:amilton.junior@usp.br)

 Supplemental data for this article can be accessed <https://doi.org/10.1080/09593330.2022.2031312>.

© 2022 Informa UK Limited, trading as Taylor & Francis Group

development were included – no poverty and hunger, education, gender quality, sanitation, clean water and energy, decent work related to economic growth and inequalities reduction, industrial innovations, sustainable city and responsible consumption, life on land and below water, justice and international partnership [1–4].

Despite the several efforts, the pollution by metallic species from industrial activities, such as mining and electroplating, is still a crucial concern considering the negative impacts on the environment and human health [5–9]. Copper, zinc, cobalt, and nickel are a few examples of metals widely used in our daily life, mainly in electroplating industries [9,10]. Many techniques have been applied for wastewater treatment to remove/recover metallic ions, such as ion exchange resins [11], precipitation [12], zeolites [9], nanomaterials [13,14] and biosorbents [15,16].

In the case of biosorbents, biotechnology is focused on microorganism abilities for metallic ions adsorption from contaminated effluents. The literature has demonstrated the high capacity of such material for wastewater treatment compared to commercial sorbents [17]. Furthermore, these microorganisms can be obtained from different sources, such as mining [18].

Different biomass can be used, such as algae [19], yeasts [20], microalgae [17], fungi [21], and bacteria [10], and both dead or living cells are capable of adsorbing metallic ions [15]. As a result, the wastewater treatment using biomass saves energy and costs, minimizes chemical sludge volumes, highly selective and efficient rates, even in low concentrations. By the same token, water can be reused after the removal of metallic ions, declining its consumption and the pressure on the environment [20,22]. After the adsorption process, it is possible to obtain the metals from the biomass, allowing obtaining two streams: water treated and metallic ions with important value.

The present study has as a novelty the use of bacterial biomass obtained from a contaminated area (Cubatão – SP – BR) for metallic ions adsorption, demonstrating that it is possible to have a low-cost material for industrial wastewater treatment. The city is known by the variable industries that historically impacted air, water, and soils through industrial pollution from their activities and environmental negligence. All these factors were important to determine the local for sample withdrawal.

The bacteria presented in the sample were isolated and identified by the MALDI-TOF technique. The microorganism was grown in LB culture medium and further submitted to the lyophilization process. Adsorption experiments were carried out on a fixed-bed column using lyophilized biomass. It was evaluated the

adsorption capacity of zinc (Zn) and copper (Cu) simulating an industrial wastewater. Both contaminants are widely presented in waste water of electroplating processes [23–26]. Activated charcoal was tested to compare with the lyophilized biomass. Adsorption isotherms were applied to determine the behaviour of the adsorption phenomenon. At some degree, the subject of the present study addressed here strongly linkages with specifically targets 6.3, 8.4, 9.4 and 12.4 of the SDGs [1]. To the best of our knowledge, no study in the literature has correlated it with wastewater treatment using microbial biomass from a contaminated area.

## 2. Materials and methods

### 2.1. Materials

#### 2.1.1. Collecting soil samples

Samples were withdrawal from Cubatão city (São Paulo – Brazil) in the area of the Environment Research Center (CEPEMA – University of Sao Paulo) – 23°53'13"S 46° 26'15"W. Figure S1 shows the sample collection point. Two samples were collected in March/2017; about 80 g of soil was collected after digging 10 cm deep and stored in a cold chamber at 4°C [27].

#### 2.1.2. Biomass preparation

The microbial cultivation was carried out using 5 g of the soil collected in 150 mL of Erlenmeyer flasks with 100 mL of LB medium (Lysogeny Broth) composed of 10 g/L peptone, 5 g/L yeast extract, and 10 g/L NaCl [10]. The microorganisms were kept under constant agitation on an orbital shaker at 180 pm, at  $28 \pm 2^\circ\text{C}$  for 48 h for the biological growth.

Then, a volume of 20 mL of culture sample was added into 1L of Erlenmeyer flask with 700 mL of LB medium for subculture, repeated until the amount of biomass for the experiments. Samples were stored in Eppendorf microtubes at  $-80^\circ\text{C}$ . After the growth phase, the culture sample was collected and centrifuged at 10,000 rpm (HITACHI CR 22N – 16800 RCF) for 5 min. The solid phase was washed with 0.9% NaCl solution and further stored at  $-20^\circ\text{C}$ .

The resulting biomass was prepared following the steps of lyophilization, comminution, and autoclaving. First, the biomass was stored at  $-80^\circ\text{C}$  for 48 h, the sample was exposed to the lyophilization process for 72 h (Liobrás LioTop – L101) at  $-60^\circ\text{C}$  and  $<500\text{mmHg}$ . After comminuting using mortar and pistil, the biomass was autoclaved at  $121^\circ\text{C}$  for 20 min. Before the fixed-bed experiments, the material was dried at  $105^\circ\text{C}$  for 24 h.

### 2.1.3. Characterization of biomass

The bacteria isolation was carried out using the samples collected during the microorganism's growth, as described by Avanzi et al. [18]. To sum up, samples were added in Petri dishes previously prepared with agar autoclaved for 120 min at 121°C for incubation in an oven for 48 h at 37°C. Using sterile plastic rods, samples of these colonies were collected and deposited in a new conical flask with culture medium for growth of this target colony, for a new growth cycle at 180 rpm, 28°C for 48 h. The procedure was repeated until achieving a homogeneous colony [18].

So, samples were taken and transferred to the polished steel target plates followed by the addition of 1 µL of α-cyano-4-hydroxycinnamic acid in saturated solution with 50% acetonitrile and 2.5% trifluoroacetic acid (TFA). The analyses were carried out in triplicate in MALDI-TOF equipment (Bruker Daltonics, Microflex LT model). The spectra were evaluated in Biotyper 3.0 software compared with a reference database spectra from FlexControl 3.0 software. The classification is based on scores that express the reliability of identification that ranges from 0 to 3, where values less than 1.55 are considered as low identification profile with the reference of the spectrum library. Scores ranging from 1.55–1.9 indicate compatibility with the genus. Values greater than 1.9 are considered reliable identification for the species.

SEM (Phenom equipment, proX model) analyses were carried to evaluate the morphology of the biomass. FT-IR (Bruker Tensor 27 IR equipment) analyses were carried to identify the molecular bonds involved in the metallic adsorption through the samples' absorbance spectra from the stage before and after adsorption/elution experiments.

## 2.2. Methodology

### 2.2.1. Synthetic solutions

Monoelementary solutions were prepared using sulfate salts of Zn ( $\text{ZnSO}_4 \cdot 7\text{H}_2\text{O}$ ) and Cu ( $\text{CuSO}_4 \cdot 5\text{H}_2\text{O}$ ) in ultra-pure water. Solutions in different were prepared for the experiments (10, 25, 50, 75, 100, 125, 150 mg/L e 175 mg/L). During the experiments, the pH was maintained at 5.4 using HCl or NaOH 1 mol/L, avoiding Zn and Cu precipitation [28,29]. The experimental error was calculated by repeating experiments, and the values were lower than 5% [3,10,30].

### 2.2.2. Biomass experiments

Adsorption experiments were carried out in fixed-bed columns with 25 cm of high, 5 cm outside diameter, and 2 cm inside diameter. In each experiment, the

columns were first loaded with 60 glass spheres of 4 mm in diameter so that there was greater porosity in the passage bed and a better contact surface. Then, the pre-defined quantity of biomass was loaded into the column. Thereby, the solution was fed (20 mL) into the column upflow using the peristaltic pump with a constant flow of 2.5 mL/min at 25°C. Samples before and after biomass adsorption were analyzed in ICP-OES (Varian 720-ES model). Equation 1 was used to calculate the percentage of metallic ions adsorbed, where %S is the percentage of ions adsorbed and  $C_0$  and  $C_e$  are ion concentration at the beginning and in the equilibrium (mg/L), respectively [11].

$$\%S = \frac{C_0 - C_e}{C_0} \times 100\% \quad (1)$$

In the present study, the column's amount of biomass was studied: 1, 0.8, and 0.5 g. The metallic ion concentration was also evaluated, ranging from 10 mg/L to 175 mg/L for solutions containing Zn and from 10 mg/L to 150 mg/L for solutions containing Cu, concentrations at which saturation was reached for metals.

After adsorption experiments, the elution step was evaluated using an acid solution to recover Zn and Cu adsorbed by the biomass at a constant 2.5 mL/min flow. HCl 0.2M and  $\text{HNO}_3$  0.2M were studied for both metallic ions. The solution during the elution process was analyzed in ICP-OES.

### 2.2.3. Activated charcoal

Activated charcoal was used to compare biomass since it is used for the industrial wastewater treatment, as most usual and accessible commercial adsorbent. The material used was of high purity without any chemical or thermal treatment before the adsorption experiment. The experiments were carried out as well as biomass experiments. Samples were analyzed in ICP-OES.

## 2.3. Adsorption isotherms

Five different adsorption models were tested: Langmuir, Freundlich, Lineweaver–Burk, Eadie–Hofstee, and Scatchard. The isotherms and the linear equations are presented in Table S1. Langmuir isotherm was developed to represent the chemisorption for a homogeneous surface. As there is a limited number of sites, the adsorption rate increases proportionally with the solute concentration. It maintains a constant value when close to the maximum number of available sites. The equilibrium condition is reached where desorption and adsorption rate in the system equalize and stabilize, and monolayers are formed [31].

Lineweaver–Burk, Eadie–Hofstee, and Scatchard are different linear equations of the Langmuir model. These linear regressions result in different parameter estimates depending on which of the linearized forms the results are adjusted since each of these variations changes the original error distribution order. Such equations from the Langmuir isotherm are important to describe the behaviour of the bonds [32–34].

The Freundlich model is an empirical equation that assumes an almost infinite number of adsorption sites due to a heterogeneous surface in terms of adsorptive energies. In response to the numerous sites, it is adopted in this model that the ions are infinitely accumulated on the adsorbent's surface, forming multilayers of adsorption [35].

As presented in Table S1,  $K_L$  is the Langmuir constant (L/mg),  $C_e$  is ion concentration in the equilibrium (mg/L) as presented in Equation 1,  $q_e$  is the amount of solute adsorbed in equilibrium (mg/g) calculated as expressed in Equation 2,  $Q_{\max}$  is the maximum capacity of ions adsorbed per mass of adsorbent (mg/g), and  $K_F$  is the Freundlich constant (L/mg) [11].

$$q_e = \frac{(C_e - C_0) \cdot V}{m_r} \quad (2)$$

### 3. Results and discussion

#### 3.1. Biomass identification from an area polluted by industrial activity

The isolated strain from the area known for pollution caused by industrial activities was identified by MALDI-TOF mass spectrometry using the Biotyper 3.0 software. Two different bacteria were isolated (Figure S2), and the analyzes indicated the presence of the following microorganism: *Enterococcus faecalis* (Figure S2A) e *Pseudomonas aeruginosa* (Figure S2B).

The MALDI-TOF spectra acquired from the strain obtained a score of 2.24 for *Enterococcus faecalis* and 2.17 for *Pseudomonas aeruginosa* from the database, indicating reliability in determining the species analyzed according to the manufacturer. Figure S3b shows the morphology of the biomass after lyophilization and comminution used in the adsorption experiments. It is possible to see the irregular and porous surface (highlighted in the SEM images) as well as regular surfaces. This fact is important for adsorption experiments, since the porous surface increases the contact surface and, consequently, the adsorption capacity [31].

*Enterococcus faecalis* is a gram-positive bacterium present in rainwater, soil, and mammals' intestines. It is pathogenic and causes infections and diarrhea in a

weakened organism. In water bodies, these species are considered indicator bacteria for the level of contamination and *E. coli* and are resistant to environmental variations and some drugs [36]. *Pseudomonas aeruginosa*, on the other hand, is a gram-negative bacterium present mainly in soils. It is an opportunistic microorganism that causes infections in the respiratory system and is the main cause of ear infection [37].

Both bacteria are abundant in the environment, easily adapt and have the characteristic of producing biofilm and were used in studies of adsorption of metals. The presence of peptidoglycans in the cell membrane makes the metallic ions recovery possible [37].

#### 3.2. Adsorption and elution experiments

##### 3.2.1. Adsorption efficiency

Experiments were performed at 25°C and pH 5.4 in fixed-bed columns with 25 cm of high, 5 cm outside diameter, and 2 cm inside diameter. A volume of 20 mL of the solution with metallic ions was fed into the column at 2.5 mL/min. The concentration of metallic ions was studied from 10 ppm to 150 ppm (Cu) and 175 ppm (Zn). Figure 1 shows Zn adsorption's efficiency by the biomass and its capacity varying the metallic ions concentration for each amount of biomass.

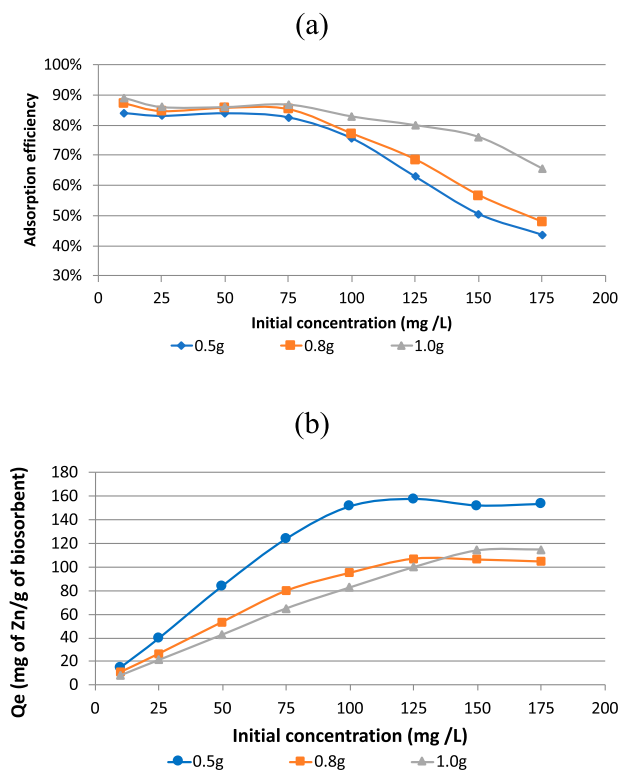


**Figure 1.** (a) adsorption efficiency and (b) adsorption capacity varying the initial Zn concentration for each amount of biomass (0.5, 0.8, and 1.0 g).



As the Zn concentration increases, the adsorption efficiency decreased independent of the amount of biomass, suggesting that the amount of available active sites is being occupied and the supply of these sites does not keep up with the increased demand for free ions in the solution [38]. Between 10 – 75 mg/L, the adsorption efficiency remained over 82%, indicating the maximum Zn adsorption by the biomass. The biomass was capable to remove up to 80% of Zn ions until 100 mg/L, and then declined due to saturation of active sites. Experiments carried out at 175 mg/L (Figure 1a) demonstrated that the Zn adsorption was higher for 1 g of biomass than 0.5 g or 0.8g.

As observed in Figure 1b, the adsorption follows the availability of sites for the occupation of the solution ions, and the adsorption capacity increased until it reaches the plateau around 125 – 175 mg/L, demonstrating the active sites were saturated. Since the amount of metal in the solution increases, the number of active sites remains unchanged, giving evidence of the adsorption process's behaviour with finite sites.

Bhattacharya et al. [39] reported such behaviour, where different adsorbent materials – as rice husk ash, activated alumina, and clarified sludge – were tested for Zn removal varying concentration from 3 to 50 mg/L. The authors claimed that the increase in the ratio between the initial metallic concentration and the amount of adsorbent causes the energetic sites to saturate, leaving low attraction energy sites resulting in a decrease in the removal efficiency [39].

The data for Cu adsorption is presented in Figure 2. The adsorption efficiency of Cu was lower than Zn, were achieved 83%, 75%, and 71% in experiments carried out at 10 mg/L using 1, 0.8, and 0.5 g of biomass (Figure 2a), and decreased as the Cu concentration increases. As observed in Zn experiments, the use of 1 g of biomass resulted in higher metallic ions adsorption. Figure 2b showed that the increase in metallic ions concentration increased the adsorption capacity, as the number of activity sites increased, and reached the plateau in Cu concentration of 125 mg/L, indicating the activity sites were saturated. According to the literature, it occurs due to a possible dissimulative effect that resembles the affinity between adsorbent/adsorbate, but which is caused by the variation in concentration (diffusion gradient) [40,41].

The adsorption efficiency in the experiment performed with 25 mg/L of Cu and 1 g of biomass was 81%, and the adsorption capacity was 20 mg Cu/g biomass. However, when at an initial concentration of 125 mg/L and the same mass of adsorbent, the values of metallic ions removal and adsorption capacity were

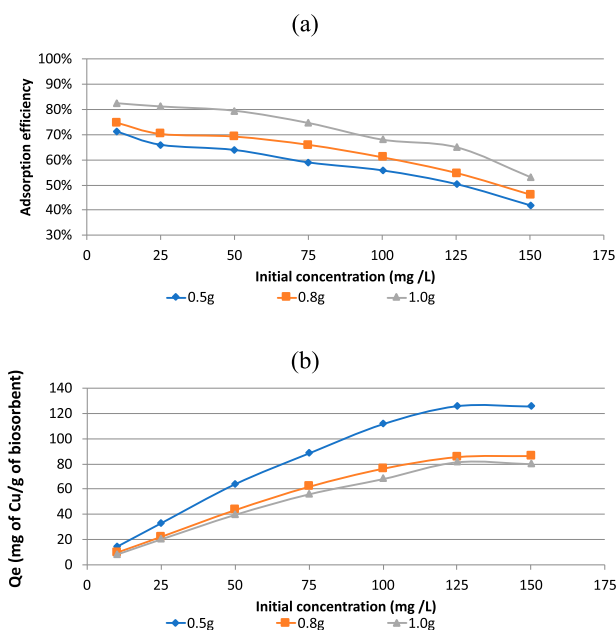


**Figure 2.** (a) adsorption efficiency and (b) adsorption capacity varying the initial Cu concentration for each amount of biomass (0.5, 0.8, and 1.0 g).

65% and 81 mg of Cu/g biomass, respectively, due to the diffusion gradient effect as aforementioned [40,41].

### 3.2.2. Elution experiments

The desorption of metallic ions was performed using HNO<sub>3</sub> and HCl 0.2M. Figure S4 shows the elution efficiency from the biomass after adsorption of Zn (a) and Cu (b) by HCl and HNO<sub>3</sub>. The highest desorption rates were obtained by HNO<sub>3</sub> – up to 95% for Zn and 83% for Cu.

Moreover, the difference between HCl and HNO<sub>3</sub> is clearly observed for Zn concentrations above 50 mg/L. HNO<sub>3</sub> elution achieved the plateau at 100 mg/L of Zn for all biomass amounts, while HCl elution kept declining as the metallic ion concentration increased, achieving efficiencies lower than 53%. It corroborates with FT-IR analysis data.

HNO<sub>3</sub> acid solution acts in the electromagnetism of the active sites releasing H<sup>+</sup> ions in the solution, weakening the attraction force between metal and the biomass as the competition for active sites increases to causing oxidation of the molecules available on the surface of the adsorbent material. These aspects help to remove the metal adsorbed on the biomaterial [32].

Also, the elution experiment carried out using HCl for 1 g of biomass achieved similar rates of HNO<sub>3</sub> in comparison with 0.8 and 0.5 g, in experiments performed using 10-50 mg/L of Zn and in all Cu concentrations. It occurs because the highest amount of adsorbent increases the number of activity sites, resulting in metals' greater

adsorption. However, in Zn concentrations above 50 mg/L, HCl achieved lower efficiencies than  $\text{HNO}_3$ .

### 3.2.3. FT-IR analysis of the biomass in adsorption

The FT-IR spectra of biomass before and after Zn and Cu adsorption and elution by 0.2M HCl and  $\text{HNO}_3$  identified the peaks:  $500\text{cm}^{-1}$ ,  $1080\text{cm}^{-1}$ ,  $1250\text{cm}^{-1}$ ,  $1350\text{cm}^{-1}$ ,  $1400\text{cm}^{-1}$ ,  $1540\text{cm}^{-1}$ ,  $1640\text{cm}^{-1}$ , and  $3300\text{cm}^{-1}$ . The associated absorption band frequencies and functional groups are presented in the **Supporting Material**.

There are amines, carboxylic acids, and phosphates in the biomass, compounds that are part of the composition of proteins and polysaccharides [42]. Peaks in the  $500\text{cm}^{-1}$  region indicate the presence of sulfur molecules and a trace of the polysaccharides'  $\text{CH}_2$  vibration, whereas the peaks of  $1080\text{cm}^{-1}$  and  $3300\text{cm}^{-1}$  suggest the vibration of species with hydroxyls present in alcohols and acids carboxylic acids [43]. Usual in vibrations of functional groups such as ketones and carboxylic acids are detectable in the peaks located in  $1250\text{cm}^{-1}$  and  $1640\text{cm}^{-1}$  present in the sample spectrum, already peaks in regions of  $1500\text{--}1600\text{cm}^{-1}$  indicate amines (proteins and peptides) [42].

The FT-IR data for Zn adsorption showed that the polysaccharides and phosphates ( $500\text{cm}^{-1}$ ), carbon-chain ( $1350\text{cm}^{-1}$ ), amines ( $1540\text{cm}^{-1}$  and  $3300\text{cm}^{-1}$ ), the carboxylic acid ( $1640\text{cm}^{-1}$ ), and alcohol ( $3300\text{cm}^{-1}$ ) might be the main chemical species involved in the metal adsorption phenomenon. For Cu adsorption, it was also observed the involvement of phosphodiesteres ( $1400\text{cm}^{-1}$ ) in ions adsorption.

The presence of polysaccharides and vibrations of hydrocarbons, in addition to the formation of the characteristic peaks of hydroxyls, carbonyls, amines, and carboxyls, correspond to those present in biopolymers, which are part of cell walls, such as saccharides and peptides (cellulose, lignin, and pectin) [44]. It is possible to notice that there are indications of higher vibrations of these species before adsorption than the spectrum after the adsorptive activity.

The elution data suggest that the metallic ions eluted and that the molecular vibrations at the active sites have returned to the initial state [42]. After elution in Zn adsorption, the FT-IR spectra show the same peaks of raw biomass for  $\text{HNO}_3$ , while biomass after HCl elution indicates changes in absorbance in the range of  $1080\text{cm}^{-1}$  to  $1640\text{cm}^{-1}$ . For FT-IR spectra after elution in Cu adsorption, it was observed a difference in absorbance at  $1350\text{cm}^{-1}$  using  $\text{HNO}_3$  and at  $500\text{cm}^{-1}$  and  $3300\text{cm}^{-1}$  using both acids.

As a result, FT-IR analysis concludes that  $\text{HNO}_3$  is the best eluting agent compared to HCl for Zn and Cu removal from the biomass. The data shows that, after

the desorption of Cu and Zn ions, the active sites' structure and properties remained stable, even suggesting reuse of biosorbent in an effective new adsorption phase. It will help the economic aspect of commercial application [12]. Zhang and Wang found similar behaviour (2015) regenerating an adsorbent material (lignocellulose) using  $\text{HNO}_3$  0.2M for nickel removal, where the sorption capacity remained after five sorption-desorption cycles [45]. The same was observed by Perez et al. (2020) using commercial material [12].

The biomass after  $\text{HNO}_3$  elution remained the same peaks of raw biomass, mainly  $1540\text{cm}^{-1}$  and  $1640\text{cm}^{-1}$ , unlike HCl experiments. It shows that the HCl solution could not elute Zn ions from amines and carboxylic acid functional groups, indicating a strong link between these ions and the functional groups. Comparing to the Cu experiments, the opposite was observed. Both  $\text{HNO}_3$  and HCl did not elute Cu ions from the phosphorus and sulfur ( $500\text{cm}^{-1}$ ) and alcohol/amines ( $3300\text{cm}^{-1}$ ) functional groups. For this reason, the elution efficiency rates were pretty much similar.

### 3.2.4. Comparison of biomass and activated charcoal on Zn and Cu adsorption

The comparison between biomass and activated charcoal for Zn and Cu adsorption was carried out to compare the material here studied with a material widely used in industrial applications. Figure 3 shows the adsorption capacity of activated charcoal and biomass. As the metallic ion concentration increased, the adsorption capacity also increased.

The biomass achieved better results for Zn adsorption than charcoal – for the experiment performed using 175 mg/L, the removal rates were 42% and 66% for activated charcoal and biomass, respectively. In the same experiment, the final solution after charcoal treatment had 100 mg/L of Zn, while after biomass treatment, the concentration was 60 mg/L. It shows that the biomass is more efficient and sustainable than one of the most

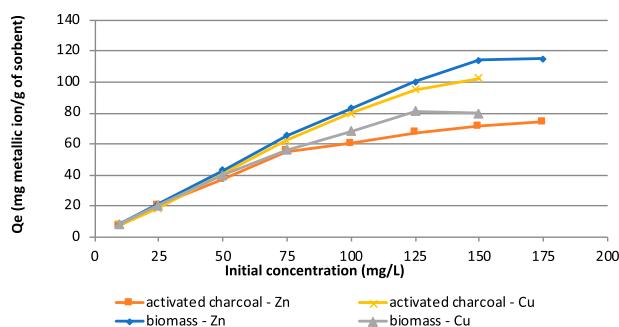


**Figure 3.** Comparison of activated charcoal and biomass on Zn and Cu adsorption varying the metallic ion concentration using 1 g of sorbent.

commercial sorbents for industrial treatment. After 75 mg/L of Zn, the formation of a plateau is observed for charcoal, formed after 150 mg/L using biomass.

According to Ramos et al. (2002), who achieved a removal rate of 50 mg of Zn/g of activated carbon at pH below 7, there is the creation of a repulsion condition between the coal and the Zn ions, because, with the pH below from the isoelectric point (equilibrium point of positive and negative charges between the species involved in the interaction), it is possible that the cases of ion retention occurred due to chemical attraction and not electrostatic attraction [46].

In the case of Cu, activated charcoal achieved better results than the biomass. For the experiment performed using 150 mg/L, the removal rates were 68% and 47% for activated charcoal and biomass, respectively – 48 and 70 mg/L of Cu in the solution treated by these adsorbents. The difference between Zn and Cu adsorption might be explained due to the affinity of activated charcoal by Cu ions by the functional groups present on the surface formed during the activation of the material [47].

According to the comparison between biomass from an area polluted by industrial activity and the commercial sorbent (activated charcoal), it is possible to state that the biomass may be used for treatment of wastewater contaminated with metallic ions (Zn and Cu). Although the adsorption efficiency for Cu was lower than activated charcoal, the biomass experiments' results were substantial. Moreover, sustainable relevance would make the biomass even more attractive.

### 3.3. Isotherms for Zn and Cu adsorption

Langmuir, Lineweaver–Burk, Eadie–Hofstee, Scatchard, and Freundlich isotherms were studied to comprehend the adsorption of Zn and Cu onto biomass. The

equations are presented in Table S1. The metallic ion concentration was varied, and the amount of biomass was 1 g. Isotherms were plotted and are presented in **Supplementary material**.

Results for Zn adsorption indicated that Lineweaver–Burk isotherm ( $r^2 = 0.9955$ ) fits better than Freundlich ( $r^2 = 0.9270$ ). The comparison of isothermal models in a non-linearized form with empirical data is presented in Figure S7, where it is clearly demonstrated that the best fit to the Lineweaver–Burk model and indicating a possible phenomenon occurring in a monolayer, where the sites are equally energetic and do not interfere with the neighbouring site. Lin and Lai [48] obtained similar achievements for *Pseudomonas aeruginosa* bacteria applied for Pb adsorption and regenerated with 0.1M HCl [48]. By the same token, Bhattacharya et al. [39] found similar results for Zn adsorption using waste materials where clarified sludge achieved best results [39]. A few examples from the literature is presented in Table 1.

The  $Q_{max}$ , according to the Lineweaver–Burk, is 200.3 mg of Zn per gram of biomass. The value of the coefficient  $n$  calculated in the Freundlich model indicates the process's spontaneity, where this constant greater than 1 indicates that the process is spontaneous [49]. The data for Zn adsorption demonstrated that the process is thermodynamic feasible and, the higher the initial metallic concentration, the tendency for an irreversible process to occur also increases.

This behaviour is due to the intraparticle diffusion force of ions in the pores of the biosorbent that is proportional to the increase in the concentration of ions in the solution, forced by the diffusion gradient, a force resulting from the differential of the concentration of metal ions in the solution and within the adsorbent. The force of attraction and desorption is influencing

**Table 1.** A comparative for Cu and Zn adsorption by different materials/techniques compared with the present study.

Adsorbent material	Functional group	Time	pH	Mass of material	Temperature	Isotherm	Kinetic model	References
Biomass (Cu and Zn)	(see Table 2 in Supporting material)	Continuous process	5.4	1.0g	25°C	Zn - Lineweaver-Burk model Cu - Langmuir model	–	Present study
Rice husk ash, clarified sludge, neem bark and activated alumina (Zn)	Biomass	60min	5.0	1.0g	30°C	Langmuir and Freundlich	First-order Lagergren rate	[39]
Biomass (Zn)	<i>Pseudomonas aeruginosa</i>	60min	7.7	10 mL of cell suspensions	26–30°C	Langmuir	–	[51]
Biomass (Cu)	<i>Rhodococcus erythropolis</i>	20min	6.0	1.0 g/L	–	Langmuir	–	[10]
Dowex XUS 43605 (Cu)	HPPA	120min	1.5	1.0g	25–35°C	Langmuir	Pseudo-second order	[52]
Dowex M4195 (Cu)	Bisepicolylamine	410min	1.3	2.0g	–	Langmuir	Pseudo-second order	[53]
Lewatit TP 207 (Cu)	Iminodiacetate	180min	2.0	1.17g	25°C	Langmuir	–	[49]
Sodium dithionite (Cu)	–	45min	0.5	–	25°C	–	–	[12]



the ions by the 'biosorbent – solution' system according to the concentration of the metallic solution [50].

Their linearized form indicated a better fit of Cu adsorption results in the Langmuir model ( $r^2 = 0.9908$ ). The data from the experiments are very congruent with the curves of the Langmuir models. Pérez Silva et al. [51] studied the microorganism *Pseudomonas aeruginosa* in the biosorption of Cu and Zn, where the adsorption followed the Langmuir model (Table 1) [51]. The  $Q_{\max}$  calculated for Cu adsorption was 164.16 mg of Cu per gram of biomass. The value of the coefficient  $n$  found in the Freundlich model also indicates the process's spontaneity, with a value of 1.5835.

#### 4. Conclusion

The present study aimed to use biomass from an area polluted by industrial activity for the adsorption of metallic ions in a fixed-bed reactor on a laboratory scale. The cultivation of the microorganisms in LB medium and further analysis in MALDI-TOF equipment showed *Enterococcus faecalis* and *Pseudomonas aeruginosa*. It occurs due to the known history of industrial contamination in the region where the samples were taken. Adsorption experiments of Zn and Cu metallic ions showed efficiency rates above 50% and up to 90%. Comparing with activated charcoal, biomass achieved higher efficiency for Zn but slightly below for Cu. Despite that, the results achieved were similar to different biosorbents and commercial sorbents. Desorption experiments using different acid solutions showed that  $\text{HNO}_3$  reached better efficiency than HCl since  $\text{HNO}_3$  acid solution acts in the electromagnetism of the active sites releasing  $\text{H}^+$  ions in the solution, increasing the competition between such ions and metallic ions. Zn adsorption fitted better for the Lineweaver–Burk model, while Cu adsorption by the biomass fitted better for Langmuir. The theoretical rates of maximum removal were 200 mg/g of biomass for Zn and 164 mg/g of biomass for Cu. This contribution fits the goals of the United Nations Sustainable Development Goals (targets 6.3, 8.4, 9.4 and 12.4).

#### Disclosure statement

The authors declare that they have no known competing financial interests or personal relationships that could have appeared to influence the work reported in this paper.

#### Funding

This work was supported by São Paulo Research Foundation: [Grant Number 2012/51871-9 and 2019/11866-5].

#### Data availability statement

The data that support the findings of this study are available from the corresponding author, A.B. Botelho Junior, upon reasonable request.

#### ORCID

Amilton Barbosa Botelho Junior  <http://orcid.org/0000-0002-3421-6286>

Denise Crocce Romano Espinosa  <http://orcid.org/0000-0003-2359-9485>

Jorge Alberto Soares Tenório  <http://orcid.org/0000-0002-7849-7470>

#### References

- [1] United Nations. Global indicator framework for the Sustainable Development Goals and targets of the 2030 Agenda for Sustainable Development [Internet]. 2020 [cited 2021 Jan 8]. p. 21. Available from: [https://unstats.un.org/sdgs/indicators/GlobalIndicatorFrameworkafter2019refinement\\_Eng.pdf%0Ahttps://unstats.un.org/sdgs/indicators/GlobalIndicatorFramework\\_A.RES.71.313Annex.pdf](https://unstats.un.org/sdgs/indicators/GlobalIndicatorFrameworkafter2019refinement_Eng.pdf%0Ahttps://unstats.un.org/sdgs/indicators/GlobalIndicatorFramework_A.RES.71.313Annex.pdf).
- [2] Botelho Junior AB, Espinosa DCR, Vaughan J, et al. Recovery of scandium from various sources: A critical review of the state of the art and future prospects. Miner Eng [Internet]. 2021;172:107148. Available from: <https://linkinghub.elsevier.com/retrieve/pii/S0892687521003770>.
- [3] Botelho Junior AB, Espinosa DCR, Tenório JAS. Selective separation of Sc(III) and Zr(IV) from the leaching of bauxite residue using trialkylphosphine acids; tertiary amine, tri-butyl phosphate and their mixtures. Sep Purif Technol [Internet]. 2021;279:119798. doi:10.1016/j.seppur.2021.119798.
- [4] Martins LS, Guimarães LF, Botelho Junior AB, et al. Electric car battery: An overview on global demand, recycling and future approaches towards sustainability. J Environ Manage [Internet]. 2021;295:113091. doi:10.1016/j.jenvman.2021.113091.
- [5] Santander P, Morales D, Rivas BL, et al. Removal of Cr(VI) from aqueous solution by a highly efficient chelating resin. Polym Bull. 2017;74:2033–2044.
- [6] Zhao M, Xu Y, Zhang C, et al. New trends in removing heavy metals from wastewater. Appl Microbiol Biotechnol [Internet]. 2016;100:6509–6518. doi:10.1007/s00253-016-7646-x.
- [7] Ali H, Khan E, Ilahi I. Environmental chemistry and ecotoxicology of hazardous heavy metals: environmental persistence; toxicity, and bioaccumulation. J Chem. 2019: 1–14.
- [8] Tayebi-Khorami M, Edraki M, Corder G, et al. Re-thinking mining waste through an integrative approach Led by circular economy aspirations. Minerals [Internet]. 2019;9:286. doi:10.3390/min9050286.
- [9] Izidoro JC, Kim MC, Bellelli VF, et al. Synthesis of zeolite A using the waste of iron mine tailings dam and its application for industrial effluent treatment. J Sustain Min [Internet]. 2019;18:277–286. Available from: <https://linkinghub.elsevier.com/retrieve/pii/S2300396019301119>.

- [10] Baltazar MDPG, Gracioso LH, Avanzi IR, et al. Copper bio-sorption by *Rhodococcus erythropolis* isolated from the Sossego Mine - PA - Brazil. *J Mater Res Technol* [Internet]. 2019;8:475–483. doi:10.1016/j.jmrt.2018.04.006.
- [11] Botelho Junior AB, Vicente ADA, Espinosa DCR, et al. Recovery of metals by ion exchange process using chelating resin and sodium dithionite. *J Mater Res Technol* [Internet]. 2019;8:4464–4469. Available from: <https://linkinghub.elsevier.com/retrieve/pii/S2238785418312110>.
- [12] Perez ID, Anes IA, Botelho Junior AB, et al. Comparative study of selective copper recovery techniques from nickel laterite leach waste towards a competitive sustainable extractive process. *Clean Eng Technol* [Internet]. 2020;1:100031. Available from: doi:10.1016/j.clet.2020.100031%0Ahttps://linkinghub.elsevier.com/retrieve/pii/S2666790820300318.
- [13] Malakootian M, Khatami M, Mahdizadeh H, et al. A study on the photocatalytic degradation of p-Nitroaniline on glass plates by Thermo-Immobilized ZnO nanoparticle. *Inorg Nano-Metal Chem* [Internet]. 2020;50:124–135. Available from: doi:10.1080/24701556.2019.1662807.
- [14] Javid N, Malakootian M. Removal of bisphenol a from aqueous solutions by modified-carbonized date pits by zno nano-particles. *Desalin Water Treat*. 2017;95:144–151.
- [15] Bădescu IS, Bulgariu D, Ahmad I, et al. Valorisation possibilities of exhausted biosorbents loaded with metal ions – A review. *J Environ Manage*. 2018;224:288–297.
- [16] Tan H, Wang C, Zeng G, et al. Bioreduction and biosorption of Cr(VI) by a novel *Bacillus* sp. CRB-B1 strain. *J Hazard Mater* [Internet]. 2020;386:121628. doi:10.1016/j.jhazmat.2019.121628.
- [17] Ubando AT, Africa ADM, Maniquiz-Redillas MC, et al. Microalgal biosorption of heavy metals: A comprehensive bibliometric review. *J Hazard Mater* [Internet]. 2021;402:123431. doi:10.1016/j.jhazmat.2020.123431.
- [18] Avanzi IR, Gracioso LH, Baltazar MDPG, et al. Rapid bacteria identification from environmental mining samples using MALDI-TOF MS analysis. *Environ Sci Pollut Res*. 2017;24:3717–3726.
- [19] Calfa BA, Torem ML. Bioreagents - Their use in the removal of heavy metals from liquid streams by biosorption/ bioflotation. *Rev Esc Minas* [Internet]. 2007;60:537–542. Available from: [http://www.scielo.br/scielo.php?script=sci\\_arttext&pid=S0370-44672007000300015&lng=pt&tlng=pt](http://www.scielo.br/scielo.php?script=sci_arttext&pid=S0370-44672007000300015&lng=pt&tlng=pt).
- [20] Zhang M, Wen Y, Luo X, et al. Characterization, mechanism of cypermethrin biosorption by *saccharomyces cerevisiae* strains YS81 and HP and removal of cypermethrin from apple and cucumber juices by inactive cells. *J Hazard Mater*. 2021;407(124350):1–11.
- [21] Davoodi SM, Miri S, Taheran M, et al. Bioremediation of unconventional oil contaminated ecosystems under natural and assisted conditions: A review. *Environ Sci Technol*. 2020;54:2054–2067.
- [22] Soto-Ramírez R, Lobos M-G, Córdova O, et al. Effect of growth conditions on cell wall composition and cadmium adsorption in *chlorella vulgaris*: A new approach to biosorption research. *J Hazard Mater* [Internet]. 2021;125059. doi:10.1016/j.artmed.2020.101998.
- [23] Barros KS, Martí-Calatayud MC, Scarazzato T, et al. Investigation of ion-exchange membranes by means of chronopotentiometry: A comprehensive review on this highly informative and multipurpose technique. *Adv Colloid Interface Sci*. 2021;293(102439):1–31.
- [24] Feijoo GC, Barros KS, Scarazzato T, et al. Electrodialysis for concentrating cobalt, chromium, manganese, and magnesium from a synthetic solution based on a nickel laterite processing route. *Sep Purif Technol* [Internet]. 2021;275(119192):1–10. doi:10.1016/j.seppur.2021.119192.
- [25] Scarazzato T, Panossian Z, Tenório JAS, et al. Water reclamation and chemicals recovery from a novel cyanide-free copper plating bath using electrodialysis membrane process. *Desalination* [Internet]. 2018;436:114–124. Available from: doi:10.1016/j.desal.2018.01.005.
- [26] Scarazzato T, Panossian Z, Tenório JAS, et al. A review of cleaner production in electroplating industries using electrodialysis. *J Clean Prod*. 2016;168:1590–1602.
- [27] Silvestri E, Hall K, Chambers-Velarde Y, et al. Sampling, Laboratory, and Data Considerations for Microbial Data Collected in the Field [Internet]. 2018. Available from: [https://cfpub.epa.gov/si/si\\_public\\_file\\_download.cfm?p\\_download\\_id=536543&Lab=NHSRC](https://cfpub.epa.gov/si/si_public_file_download.cfm?p_download_id=536543&Lab=NHSRC).
- [28] Jackson E. *Hydrometallurgical extraction and reclamation*. 1st ed. Southampton: Ellis Horwood Limited; 1986.
- [29] Pourbaix M. *Atlas of electrochemical equilibria in aqueous solutions* [Internet]. Second. Franklin JA, editor. Houston: National Association of Corrosion Engineers; 1974. Available from: <https://store.nace.org/atlas-of-electrochemical-equilibria-in-aqueous-solu>.
- [30] Botelho Junior AB, Pinheiro ÉF, Espinosa DCR, et al. Adsorption of lanthanum and cerium on chelating ion exchange resins: kinetic and thermodynamic studies. *Sep Sci Technol* [Internet]. 2021; 1–10. doi:10.1080/01496395.2021.1884720.
- [31] Zagorodni AA. *Ion exchange materials: properties and applications*. 1st ed. Elsevier. Stockholm: Elsevier; 2012.
- [32] Kinniburgh DG. General purpose adsorption isotherms. *Environ Sci Technol*. 1986;20:895–904.
- [33] Ho Y-S. Isotherms for the sorption of lead onto peat: comparison of linear and Non-linear methods. *Polish J Environ Stud*. 2006;15:81–86.
- [34] Cho YS, Lim HS. Comparison of various estimation methods for the parameters of michaelis-menten equation based on in vitro elimination kinetic simulation data. *Transl Clin Pharmacol*. 2018;26:39–47.
- [35] Inamuddin ML. *Ion exchange technology I* [Internet]. Dr. Inamuddin, Luqman M, editors. Dordrecht: Springer Netherlands; 2012; Available from: <http://link.springer.com/10.1007/978-94-007-1700-8>.
- [36] Yu J, Zhang D, Ren W, et al. Transport of *Enterococcus faecalis* in granular activated carbon column: potential energy, migration, and release. *Colloids Surfaces B Biointerfaces* [Internet]. 2019;183:110415. doi:10.1016/j.colsurfb.2019.110415.
- [37] Cui J, Zhu N, Kang N, et al. Biorecovery mechanism of palladium as nanoparticles by *Enterococcus faecalis*: from biosorption to bioreduction. *Chem Eng J* [Internet]. 2017;328:1051–1057. doi:10.1016/j.cej.2017.07.124.
- [38] Jeon YW. Optimization of ultrasonification of slaughter blood for protein solubilization. *Environ Eng Res*. 2015;20:163–169.

- [39] Bhattacharya AK, Mandal SN, Das SK. Adsorption of Zn(II) from aqueous solution by using different adsorbents. *Chem Eng J*. 2006;123:43–51.
- [40] Veli S, Alyüz B. Adsorption of copper and zinc from aqueous solutions by using natural clay. *J Hazard Mater*. 2007;149:226–233.
- [41] Lu W-B, Shi J-J, Wang C-H, et al. Biosorption of lead, copper and cadmium by an indigenous isolate *Enterobacter* sp. J1 possessing high heavy-metal resistance. *J Hazard Mater* [Internet]. 2006;134:80–86. Available from: <https://linkinghub.elsevier.com/retrieve/pii/S0304389405006527>.
- [42] Chubar N, Behrends T, Van Cappellen P. Biosorption of metals (Cu<sup>2+</sup>, Zn<sup>2+</sup>) and anions (F<sup>-</sup>, H<sub>2</sub>PO<sub>4</sub><sup>-</sup>) by viable and autoclaved cells of the Gram-negative bacterium *Shewanella putrefaciens*. *Colloids Surfaces B Biointerfaces*. 2008;65:126–133.
- [43] Derrick MR, Stulik D, Landry JM. Infrared spectroscopy in conservation science. Los Angeles: Getty Publications; 1999.
- [44] Vijayaraghavan K, Yun Y. Bacterial biosorbents and biosorption. *Biotechnol Adv* [Internet]. 2008;26:266–291. Available from: <https://linkinghub.elsevier.com/retrieve/pii/S0734975008000177>.
- [45] Zhang X, Wang X. Adsorption and desorption of Nickel(II) ions from aqueous solution by a lignocellulose/montmorillonite nanocomposite. *Plos One*. 2015;10:1–21.
- [46] Leyva Ramos R, Bernal Jacome LA, Mendoza Barron J, et al. Adsorption of zinc(II) from an aqueous solution onto activated carbon. *J Hazard Mater*. 2002;90:27–38.
- [47] Monser L, Adhoum N. Modified activated carbon for the removal of copper, zinc, chromium and cyanide from wastewater. *Sep Purif Technol*. 2002;26:137–146.
- [48] Lin C-C, Lai Y-T. Adsorption and recovery of lead(II) from aqueous solutions by immobilized *Pseudomonas Aeruginosa* PU21 beads. *J Hazard Mater* [Internet]. 2006;137:99–105. Available from: <https://linkinghub.elsevier.com/retrieve/pii/S0304389406002354>.
- [49] Botelho Junior AB, Vicente ADA, Espinosa DCR, et al. Effect of iron oxidation state for copper recovery from nickel laterite leach solution using chelating resin. *Sep Sci Technol* [Internet]. 2020;55:788–798. Available from: <https://www.tandfonline.com/doi/full/10.1080/01496395.2019.1574828>.
- [50] Weber TW, Chakravorti RK. Pore and solid diffusion models for fixed-bed adsorbents. *AIChE J* [Internet]. 1974;20:228–238. <http://doi.wiley.com/10.1002/aic.690200204>.
- [51] Pérez Silva RM, Ábalos Rodríguez A, Gómez Montes De Oca JM, et al. Biosorption of chromium, copper, manganese and zinc by *Pseudomonas aeruginosa* AT18 isolated from a site contaminated with petroleum. *Bioresour Technol* [Internet]. 2009;100:1533–1538. doi:10.1016/j.biortech.2008.06.057.
- [52] Perez ID, Botelho Junior AB, Aliprandini P, et al. Copper recovery from nickel laterite with high-iron content: A continuous process from mining waste. *Can J Chem Eng* [Internet]. 2020;98:957–968. Available from: <https://onlinelibrary.wiley.com/doi/abs/10.1002/cjce.23667>.
- [53] Neto IFF, Sousa CA, Brito MSCA, et al. A simple and nearly-closed cycle process for recycling copper with high purity from end life printed circuit boards. *Sep Purif Technol* [Internet]. 2016;164:19–27. doi:10.1016/j.seppur.2016.03.007.